

# Large neutrino asymmetry from forbidden decay of dark matter

Debasish Borah,<sup>1,\*</sup> Nayan Das,<sup>1,†</sup> and Indrajit Saha<sup>1,‡</sup>

<sup>1</sup>*Department of Physics, Indian Institute of Technology Guwahati, Assam 781039, India*

## Abstract

Dark matter (DM), in spite of being stable or long-lived on cosmological scales, can decay in the early Universe due to finite-temperature effects. In particular, a first order phase transition (FOPT) in the early Universe can provide a finite window for such decay, guaranteeing DM stability at lower temperatures, consistent with observations. The FOPT can lead to the generation of stochastic gravitational waves (GW) with peak frequencies correlated with DM mass. On the other hand, early DM decay into neutrinos can create a large neutrino asymmetry which can have interesting cosmological consequences in terms of enhanced effective relativistic degrees of freedom  $N_{\text{eff}}$ , providing a solution to the recently observed Helium anomaly among others. Allowing DM decay to occur below sphaleron decoupling temperature, thereby avoiding overproduction of baryon asymmetry, forces the FOPT to occur at sub-electroweak scale. This leaves the stochastic GW within range of experiments like LISA,  $\mu$ ARES, NANOGrav etc.

---

\*Electronic address: [dborah@iitg.ac.in](mailto:dborah@iitg.ac.in)

†Electronic address: [nayan.das@iitg.ac.in](mailto:nayan.das@iitg.ac.in)

‡Electronic address: [s.indrajit@iitg.ac.in](mailto:s.indrajit@iitg.ac.in)

## I. INTRODUCTION

As suggested by several astrophysical and cosmological observations [1, 2], approximately 26% of the present Universe is made up of DM, the particle origin of which is not yet known. Similar observations also suggest that the baryon content of the Universe is highly asymmetric leading to the longstanding puzzle of baryon asymmetry of Universe (BAU). This observed excess of baryons over anti-baryons is quantified in terms of the baryon to photon ratio as [3]

$$\eta_B = \frac{n_B - n_{\bar{B}}}{n_\gamma} \simeq 6.2 \times 10^{-10}, \quad (1)$$

based on the cosmic microwave background (CMB) measurements which also agrees well with the big bang nucleosynthesis (BBN) estimates [1]. While the weakly interacting massive particle (WIMP) [4–9] has been the most widely studied particle DM candidate, baryogenesis/leptogenesis [10–12] are considered to be the popular explanation for the BAU. However, none of the WIMP candidates nor baryogenesis/leptogenesis framework has been verified experimentally. While WIMP can have observable scattering rate with nucleons, persistent null results at direct detection experiments [13, 14] have pushed WIMP DM to a tight corner. On the other hand, baryogenesis and leptogenesis typically remain a high scale phenomena with limited or no direct experimental detection prospects. However, depending upon the particular model, such scenarios can have promising indirect detection prospects. One such avenue is the detection of stochastic gravitational wave (GW) background, which has been utilised in several baryogenesis or leptogenesis scenarios [15–30] as well as particle DM models [28, 29, 31–46]. Another promising avenue is the signatures at CMB due to enhanced effective relativistic degrees of freedom  $N_{\text{eff}}$  in certain leptogenesis and DM models like [47–52].

If a mechanism to explain BAU also leaves a large neutrino asymmetry at low temperatures, it can have interesting implications for observations related to BBN and CMB. Although the observed BAU restricts the net lepton asymmetry around sphaleron decoupling temperature ( $T_{\text{sph}}$ ) to be of same order as  $\eta_B$ , it is possible to have a large lepton asymmetry at post-sphaleron epoch ( $T < T_{\text{sph}}$ ) if the asymmetry is stored in neutrinos<sup>1</sup>. Such large neutrino asymmetry can enhance the effective relativistic degrees of freedom  $N_{\text{eff}}$

---

<sup>1</sup> Charge neutrality of the early Universe restricts the charge lepton asymmetry to be  $\leq \eta_B$ .

which can be measured at CMB experiments [53]. Additionally, a large neutrino asymmetry can also alter the predictions of BBN with observable consequences [53–56]. A large neutrino asymmetry also allows resonant production of sterile neutrino DM via Shi-Fuller mechanism [57]<sup>2</sup>. Alternately, such asymmetries can also alter the cosmological bounds on light sterile neutrinos [59]. Large neutrino asymmetry can also have other consequences for gravitational wave, baryogenesis, [60, 61], astrophysical structure formation [62] etc.

Motivated by this, we propose a new mechanism to create such large lepton asymmetry at post-sphaleron epoch in order not to be in conflict with the observed baryon asymmetry. While it is possible to create large lepton asymmetries in individual flavours at high scale while keeping the net lepton asymmetry  $\sim \mathcal{O}(\eta_B)$  [63], there exist tight constraints on such setup due to the generation of helical hypermagnetic field which can source a new contribution to the baryon asymmetry of the Universe, as pointed out recently in [64]. Among the scenarios considered so far to generate large neutrino asymmetry, one recent attempt [65] along with a few related earlier works [63, 66, 67] have utilised the Affleck-Dine mechanism [68]. The authors of [69] considered TeV scale leptogenesis from decay and scatterings as source of such lepton asymmetry generated at low scales while also creating the required lepton asymmetry at  $T = T_{\text{sph}}$  to generate the observed BAU. In [70], a two-phase leptogenesis model was proposed where sub-electroweak scale right handed neutrino (RHN) can generate lepton asymmetries at two different scales due to finite-temperature effects on its mass. In this work, we consider the possibility of generating such large lepton asymmetry from forbidden decay of DM. Although DM is stable on cosmological scales, it can decay in the early Universe due to finite-temperature effects. Role of such forbidden DM decay on generating BAU was discussed in earlier works [29, 71]. We consider initially overproduced asymmetric DM [72–78] to be the source of such large neutrino asymmetry. The decay of DM into neutrino is facilitated by a first order phase transition (FOPT) providing a finite window in which DM can decay, while ensuring its stability at later epochs. In addition to the cosmological consequences of such large neutrino asymmetry, the FOPT at post-sphaleron epoch leads to stochastic GW in nHz-mHz ballpark capable of explaining the recent observations of pulsar timing array (PTA) like NANOGrav [79] as well.

This paper is organised as follows. In section II, we discuss the setup to implement the

---

<sup>2</sup> One may refer to a review [58] for details of these mechanisms and relevant experimental constraints.

idea. In section III, we discuss the generation of large neutrino asymmetry from forbidden decay of DM followed by brief discussion of  $N_{\text{eff}}$  due to large neutrino asymmetry in section IV. In section V, we discuss our results followed by brief remarks on possible UV completion of our basic setup in section VI. We finally conclude in section VII.

## II. THE FRAMEWORK

We first consider a minimal setup consisting of a Dirac singlet fermion  $\chi$ , two singlet scalars  $\Phi_{1,2}$  as the new degrees of freedom beyond the standard model (BSM). An unbroken  $Z_2$  symmetry under which  $\chi, \Phi_2$  are odd while all other fields are even ensures the stability of DM. The low energy effective Lagrangian is

$$-\mathcal{L} \supset (y_1 \bar{\chi} \Phi_2 \nu + \text{h.c.}) + V(\Phi_1, \Phi_2) \quad (2)$$

where  $V(\Phi_1, \Phi_2)$ , the tree level scalar potential involving the singlet scalars, is given by

$$V_{\text{tree}} \equiv V(\Phi_1, \Phi_2) = \lambda_1 \left( |\Phi_1|^2 - \frac{v_D^2}{2} \right)^2 + \mu_{\Phi_2}^2 |\Phi_2|^2 + \lambda_2 |\Phi_2|^4 + \lambda_{\Phi_1 \Phi_2} |\Phi_1|^2 |\Phi_2|^2. \quad (3)$$

In the above scalar potential  $v_D$  is the vacuum expectation value (VEV) acquired by the scalar field  $\Phi_1$  while driving the FOPT. A gauged  $U(1)_D$  symmetry is considered under which  $\Phi_1$  has charge 1. The additional gauge sector helps in achieving a strong FOPT. We also consider  $\chi, \Phi_2$  to be charged under  $U(1)_D$  with equal charge 1. This not only helps in stabilising DM, but also has interesting consequences for DM phenomenology to be discussed later. We ignore the couplings of singlet scalar with the standard model (SM) Higgs  $H$  so that they do not affect the FOPT.

We calculate the complete potential including the tree level potential  $V_{\text{tree}}$ , one-loop Coleman-Weinberg potential  $V_{\text{CW}}$ [80] along with the finite-temperature potential  $V_{\text{th}}$  [81, 82]. The thermal field-dependent masses of different particles coupled to the singlet scalar  $\Phi_1$  are incorporated in the full potential. The zero-temperature masses of DM and  $\Phi_2$  are denoted by  $m_\chi$  and  $m_{\Phi_2}$  respectively. We then calculate the critical temperature  $T_c$  at which the potential in the  $\Phi_1$  direction acquires another degenerate minima at  $v_c = \phi_1(T = T_c)$ . The order parameter of the FOPT is defined as  $v_c/T_c$  such that a stronger FOPT corresponds to a larger  $v_c/T_c$ . The FOPT then proceeds via tunneling, the rate of which is estimated by calculating the bounce action  $S_3$  using the prescription in [83, 84].

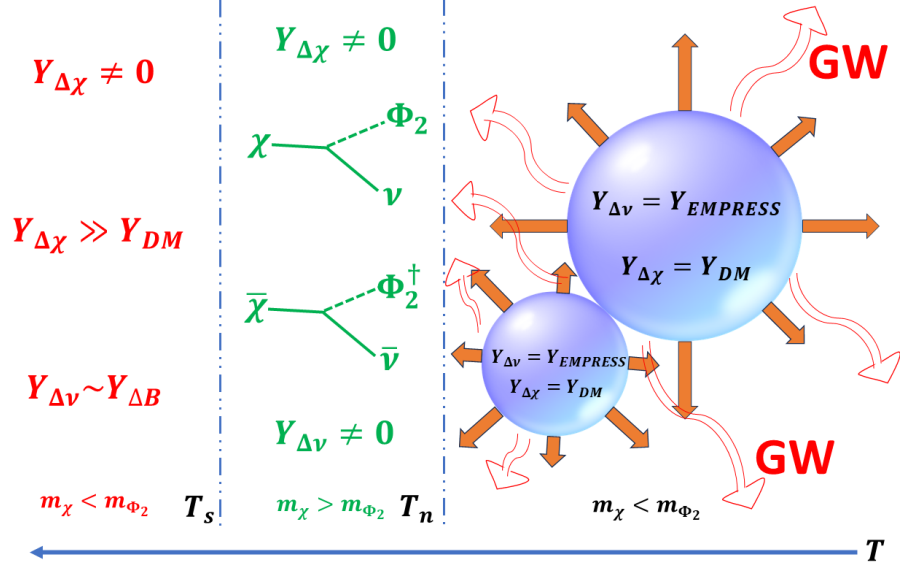


FIG. 1: The schematic diagram of co-genesis

The nucleation temperature  $T_n$  is then calculated by comparing the tunneling rate with the Hubble expansion rate of the Universe  $\Gamma(T_n) = \mathcal{H}^4(T_n)$ . We also estimate the reheat temperature  $T_{RH}$  at the end of the FOPT due to the release of radiation energy. It is defined as  $T_{RH} = \text{Max}[T_n, T_{\text{inf}}]$  [21] where  $T_{\text{inf}}$  is determined by equating density of radiation energy to that of energy released from the FOPT or equivalently  $\Delta V_{\text{eff}}$ . The details of the FOPT is given in appendix A.

We consider a large initial dark sector asymmetry  $Y_{\Delta\chi} \neq 0$  while lepton asymmetry being of the same order as baryon asymmetry to be consistent with the observed BAU. At a temperature  $T = T_s$  below the sphaleron decoupling  $T_{\text{sph}}$ , the decay of  $\chi$  into  $\Phi_2 \nu$  gets allowed enabling the transfer of dark sector asymmetry into neutrino asymmetry  $Y_{\Delta\nu}$ . At the nucleation temperature  $T = T_n$ , the decay  $\chi \rightarrow \Phi_2 \nu$  gets forbidden again due to sharp increase in  $\Phi_2$  mass. This freezes the production of neutrino asymmetry while ensuring the stability of DM at lower temperatures. Fig. 1 represents a schematic of this idea.

### III. CO-GENESIS OF LARGE NEUTRINO ASYMMETRY AND DARK MATTER

In order to calculate the final neutrino asymmetry and DM abundance starting with an initial dark asymmetry, we write the relevant Boltzmann equations for  $\chi, \nu$  and their anti-particles  $\bar{\chi}, \bar{\nu}$  together with the one for  $\Phi_2$ . We consider temperature dependent masses of relevant particles such that  $\chi, \bar{\chi}$  decay is allowed only for a finite window  $T_s > T > T_n$ . While neutrinos do not receive much thermal corrections below the electroweak scale,  $\Phi_2, \chi$  thermal masses play crucial role in determining the final asymmetries. The relevant Boltzmann equations for generating a large neutrino asymmetry from an initial dark sector asymmetry can be written as follows.

$$\begin{aligned}
\frac{dY_\chi}{dz} &= -\frac{1}{\mathcal{H}z} \langle \Gamma_\chi \rangle \Theta(m_\chi - m_{\Phi_2}) \left( Y_\chi - Y_\chi^{\text{eq}} \frac{Y_{\Phi_2}}{Y_{\Phi_2}^{\text{eq}}} \right) + \frac{1}{2\mathcal{H}z} \langle \Gamma_{\Phi_2} \rangle \Theta(m_{\Phi_2} - m_\chi) \left( Y_{\Phi_2} - Y_{\Phi_2}^{\text{eq}} \frac{Y_\chi}{Y_\chi^{\text{eq}}} \right) \\
&\quad - \frac{s}{\mathcal{H}z} \langle \sigma v_{\chi\bar{\chi} \rightarrow Z_D Z_D} \rangle (Y_\chi Y_{\bar{\chi}} - Y_\chi^{\text{eq}} Y_{\bar{\chi}}^{\text{eq}}), \\
\frac{dY_{\bar{\chi}}}{dz} &= -\frac{1}{\mathcal{H}z} \langle \Gamma_{\bar{\chi}} \rangle \Theta(m_\chi - m_{\Phi_2}) \left( Y_{\bar{\chi}} - Y_{\bar{\chi}}^{\text{eq}} \frac{Y_{\Phi_2}}{Y_{\Phi_2}^{\text{eq}}} \right) + \frac{1}{2\mathcal{H}z} \langle \Gamma_{\Phi_2} \rangle \Theta(m_{\Phi_2} - m_\chi) \left( Y_{\Phi_2} - Y_{\Phi_2}^{\text{eq}} \frac{Y_{\bar{\chi}}}{Y_{\bar{\chi}}^{\text{eq}}} \right) \\
&\quad - \frac{s}{\mathcal{H}z} \langle \sigma v_{\chi\bar{\chi} \rightarrow Z_D Z_D} \rangle (Y_\chi Y_{\bar{\chi}} - Y_\chi^{\text{eq}} Y_{\bar{\chi}}^{\text{eq}}), \\
\frac{dY_{\Phi_2}}{dz} &= \frac{1}{\mathcal{H}z} \langle \Gamma_\chi \rangle \Theta(m_\chi - m_{\Phi_2}) \left( Y_\chi - Y_\chi^{\text{eq}} \frac{Y_{\Phi_2}}{Y_{\Phi_2}^{\text{eq}}} \right) - \frac{1}{2\mathcal{H}z} \langle \Gamma_{\Phi_2} \rangle \Theta(m_{\Phi_2} - m_\chi) \left( Y_{\Phi_2} - Y_{\Phi_2}^{\text{eq}} \frac{Y_\chi}{Y_\chi^{\text{eq}}} \right) \\
&\quad + \frac{1}{\mathcal{H}z} \langle \Gamma_{\bar{\chi}} \rangle \Theta(m_\chi - m_{\Phi_2}) \left( Y_{\bar{\chi}} - Y_{\bar{\chi}}^{\text{eq}} \frac{Y_{\Phi_2}}{Y_{\Phi_2}^{\text{eq}}} \right) - \frac{1}{2\mathcal{H}z} \langle \Gamma_{\Phi_2} \rangle \Theta(m_{\Phi_2} - m_\chi) \left( Y_{\Phi_2} - Y_{\Phi_2}^{\text{eq}} \frac{Y_{\bar{\chi}}}{Y_{\bar{\chi}}^{\text{eq}}} \right), \\
\frac{dY_\nu}{dz} &= \frac{1}{\mathcal{H}z} \langle \Gamma_{\bar{\chi}} \rangle \Theta(m_\chi - m_{\Phi_2}) \left( Y_{\bar{\chi}} - Y_{\bar{\chi}}^{\text{eq}} \frac{Y_{\Phi_2}}{Y_{\Phi_2}^{\text{eq}}} \right) + \frac{1}{2\mathcal{H}z} \langle \Gamma_{\Phi_2} \rangle \Theta(m_{\Phi_2} - m_\chi) \left( Y_{\Phi_2} - Y_{\Phi_2}^{\text{eq}} \frac{Y_{\bar{\chi}}}{Y_{\bar{\chi}}^{\text{eq}}} \right), \\
\frac{dY_{\bar{\nu}}}{dz} &= \frac{1}{\mathcal{H}z} \langle \Gamma_\chi \rangle \Theta(m_\chi - m_{\Phi_2}) \left( Y_\chi - Y_\chi^{\text{eq}} \frac{Y_{\Phi_2}}{Y_{\Phi_2}^{\text{eq}}} \right) + \frac{1}{2\mathcal{H}z} \langle \Gamma_{\Phi_2} \rangle \Theta(m_{\Phi_2} - m_\chi) \left( Y_{\Phi_2} - Y_{\Phi_2}^{\text{eq}} \frac{Y_\chi}{Y_\chi^{\text{eq}}} \right).
\end{aligned} \tag{4}$$

Here  $Y_i = n_i/s$  denotes comoving number density of species “i” with  $s$  being the entropy density. Hubble expansion rate is denoted by  $\mathcal{H}$  while the variable  $z$  is  $m_\chi/T$ . The thermal averaged decay rate [11, 85] for  $\chi \rightarrow \Phi_2 \nu$  (and its conjugate) can be written as  $\langle \Gamma_\chi \rangle = \frac{y_1^2}{32\pi} \left(1 - \frac{m_{\Phi_2}^2}{m_\chi^2}\right)^2 \frac{K_1(m_\chi/T)}{K_2(m_\chi/T)}$  where  $K_{1,2}$  are modified Bessel functions of 1st, 2nd kind

respectively. Similarly,  $\langle \Gamma_{\Phi_2} \rangle = \frac{y_1^2}{16\pi} \left(1 - \frac{m_{\chi_2}^2}{m_{\Phi_2}^2}\right)^2 \frac{K_1(m_{\Phi_2}/T)}{K_2(m_{\Phi_2}/T)}$ . The  $\Theta$  functions associated with these decay widths ensures the kinematical constraints. The symmetric part of  $\chi$  can annihilate into a pair of light  $U(1)_D$  gauge bosons  $Z_D$  with  $\langle \sigma v_{\chi\bar{\chi} \rightarrow Z_D Z_D} \rangle$  denoting the corresponding thermal-averaged cross-section [86].

Next we define  $Y_{\Delta\chi} = Y_\chi - Y_{\bar{\chi}}$  and  $Y_{\Delta\nu} = Y_\nu - Y_{\bar{\nu}}$ . We choose the following initial condition for solving the above coupled Boltzmann equations

$$Y_\chi(0) = Y_\chi^{\text{eq}}, \quad Y_{\bar{\chi}}(0) = Y_\chi^{\text{eq}} - Y_{\Delta\chi}^{\text{in}} \quad (5)$$

$$Y_\nu(0) = Y_\nu^{\text{eq}}, \quad Y_{\bar{\nu}}(0) = Y_\nu^{\text{eq}}. \quad (6)$$

The initial dark sector asymmetry  $Y_{\Delta\chi}^{\text{in}}$  in required amount can be generated in a variety of ways depending upon the UV completion discussed in VI. Also, this initial DM asymmetry can be related to the origin of baryon asymmetry in the spirit of cogenesis within the framework of asymmetric dark matter (ADM) [72, 87] paradigm<sup>3</sup>.

#### IV. LARGE NEUTRINO ASYMMETRY AND $N_{\text{eff}}$

A large neutrino asymmetry can be parameterised in terms of chemical potential  $\xi$  as follows [65],

$$\eta_{\Delta L\nu} = \frac{(n_\nu - n_{\bar{\nu}})}{n_\gamma} = \frac{\pi^2}{12\zeta(3)} \sum_\alpha \xi_\alpha, \quad \alpha \equiv e, \mu, \tau, \quad (7)$$

$$Y_{\Delta\nu} = \sum_\alpha Y_{\Delta\nu\alpha} = \sum_\alpha \frac{n_{\nu\alpha} - n_{\bar{\nu}\alpha}}{s} \simeq \sum_\alpha 0.035 \xi_\alpha. \quad (8)$$

Now, the presence of neutrino asymmetry alters the energy density of neutrinos which is incorporated to the parameter  $N_{\text{eff}}$ , the effective number of relativistic species. Ignoring the effect of neutrino asymmetry on neutrino decoupling,  $\Delta N_{\text{eff}} = N_{\text{eff}} - N_{\text{eff}}^{\text{SM}}$  is given as

$$\Delta N_{\text{eff}} = \sum_\alpha \left[ \frac{30}{7} \left(\frac{\xi_\alpha}{\pi}\right)^2 + \frac{15}{7} \left(\frac{\xi_\alpha}{\pi}\right)^4 \right]. \quad (9)$$

Taking into account the effect of neutrino asymmetry on neutrino decoupling, the correction to the above expression can be written as [88]

$$\Delta N_{\text{eff}} = \sum_\alpha \left[ \frac{30}{7} \left(\frac{\xi_\alpha}{\pi}\right)^2 + \frac{15}{7} \left(\frac{\xi_\alpha}{\pi}\right)^4 + \frac{0.0102}{3} \xi_\alpha^2 \right]. \quad (10)$$

<sup>3</sup> See [74, 75] for reviews of ADM scenarios.

As this is a small correction term, both Eq. (9) and Eq. (10) give the similar change in  $N_{\text{eff}}$  in presence of neutrino asymmetry.

In the SM, such neutrino asymmetries do not arise and hence there is no additional contribution to  $N_{\text{eff}}$ . The sole contribution to  $N_{\text{eff}}$  in the SM comes from relativistic nature of light neutrinos. If neutrinos decouple instantaneously, then  $N_{\text{eff}} = 3$ . Considering non-instantaneous decoupling of SM neutrinos along with flavour oscillations and plasma correction of quantum electrodynamics, the SM  $N_{\text{eff}}$  value shifts to  $N_{\text{eff}}^{\text{SM}} = 3.045$  [89–91]. A deviation from  $N_{\text{eff}}^{\text{SM}}$  indicates presence of BSM physics either in terms of additional light degrees of freedom, new interactions of SM neutrinos or large neutrino asymmetry mentioned above. The current bound on  $N_{\text{eff}}$  from Planck 2018 data is given as  $N_{\text{eff}} = 2.99_{-0.33}^{+0.34}$  at  $2\sigma$  CL including baryon acoustic oscillation (BAO) data. This corresponds to  $\Delta N_{\text{eff}} \lesssim 0.285$ . The latest DESI 2024 data give a slightly weaker bound  $\Delta N_{\text{eff}} \lesssim 0.4$  at  $2\sigma$  CL [92]. Similar bound also exists from BBN considerations  $2.3 < N_{\text{eff}} < 3.4$  at 95% CL [93]. Future CMB experiment CMB Stage IV (CMB-S4) is expected reach a much better sensitivity of  $\Delta N_{\text{eff}} = N_{\text{eff}} - N_{\text{eff}}^{\text{SM}} = 0.06$  [94], taking it closer to the SM prediction. Another future experiment CMB-HD [95] can probe  $\Delta N_{\text{eff}}$  upto 0.014 at  $1\sigma$ .

In addition to enhancing  $N_{\text{eff}}$ , a large neutrino asymmetry can also affect the BBN predictions of light nuclei abundance, as pointed out recently in the light of anomalous observations related to primordial Helium-4 ( $^4\text{He}$ ) abundance. The recent observations made by the Subaru Survey [96], together with previous observations, have indicated a shift in primordial  $^4\text{He}$  abundance  $Y_P = 0.2379_{-0.0030}^{+0.0031}$  from the standard BBN predictions. While this is slightly smaller than earlier estimates [97–99], inclusion of the primordial deuterium constraints lead to a  $> 2\sigma$  tension between the predicted number of neutrino species  $N_{\text{eff}} = 2.41_{-0.21}^{+0.19}$  and the SM predicted value  $N_{\text{eff}} = 3.045$ , referred to as the Helium anomaly [96]. With a large neutrino asymmetry in electron flavour  $\xi_e = 0.05_{-0.03}^{+0.03}$ , it is however possible to obtain a large  $N_{\text{eff}} = 3.22_{-0.30}^{+0.33}$  consistent with SM prediction within  $1\sigma$  [96]. A combined analysis of BBN and CMB observations have also found evidence for a large neutrino asymmetry in the early Universe at  $\sim 2\sigma$  confidence level [100].



## V. RESULTS AND DISCUSSION

We first discuss the temperature dependence of relevant particle masses leading to the finite temperature window allowing forbidden decay of DM. The top panel of Fig. 2 shows temperature dependence of masses of  $\chi, \Phi_2$ . While the details of scalar masses is given in appendix A, the thermal mass of  $\chi$  [101, 102] is

$$m_\chi^2(T) = m_\chi^2 + \frac{g_D^2}{8} T^2, \quad (11)$$

with the correction being solely due to its gauge coupling. The top left and top right panel plots of Fig. 2 correspond to the benchmark points BP1, BP6 given in table I and table II respectively. Clearly, there exists a finite window  $T_n < T < T_s$  during which  $m_\chi > m_{\Phi_2}$  allowing the decay  $\chi \rightarrow \Phi_2 \nu$  and its conjugate process. We also show the sphaleron decoupling temperature  $T_{\text{sph}} \sim 130$  GeV to indicate that the large neutrino asymmetry is produced only at  $T < T_{\text{sph}}$  and hence can not get converted into baryon asymmetry. The bottom panel plots of the same figure shows the corresponding evolution of comoving number densities of  $\chi, \bar{\chi}, \Phi_2$  and  $\Delta L_\nu$ . Starting with an initial asymmetry  $Y_\chi - Y_{\bar{\chi}} \neq 0$ , the plots clearly depict the transfer of asymmetry in  $\chi$  into a neutrino asymmetry during  $T_n < T < T_s$ . For  $T < T_n$ , the neutrino asymmetry saturates while  $\chi, \bar{\chi}$  abundances continue to fall due to efficient annihilation  $\chi \bar{\chi} \rightarrow Z_D Z_D$ . Due to the finite temperature window and choice of Yukawa coupling  $y_1$  controlling the decay rate, all dark asymmetry does not get transferred to neutrinos, leaving a remnant asymmetry. The remnant asymmetric relic for the chosen benchmark points agree with the observed DM relic. Note that,  $\Phi_2$  decay for  $T < T_n$  can not alter asymmetries in dark sector or neutrinos assuming that  $\Phi_2$  does not store any asymmetry due to efficient  $\Phi_2 \rightarrow \Phi_2^\dagger$  interactions.

Fig. 3 shows the GW spectra for the benchmark points given in table I and II. The same tables also contain the details of the GW related parameters used for calculating the spectra. Clearly, the peak frequencies can remain within the sensitivity of planned future experiment like LISA [103],  $\mu$ ARES [104], THEIA [105], GAIA [105], SKA [106] and NANOGrav. The black colored violin-shaped points correspond to the recent NANOGrav data [79]. Due to the restrictions of having the FOPT below the electroweak scale, the peak frequencies do not come within reach of experiments like DECIGO [107], BBO [108] among others.

We show the summary in Fig. 4 and Fig. 5. The left panel of Fig. 4 shows the parameter space in effective Yukawa coupling  $y_1$  versus DM mass plane for benchmark

point BP1 shown in table I. Different contours correspond to different values of neutrino asymmetry. The region preferred to explain the  ${}^4\text{He}$  anomaly is shaded in blue colour. The other experimental sensitivities and Planck 2018 bounds are also shown as different coloured shades. For a fixed value of DM mass, larger  $y_1$  leads to larger neutrino asymmetry as more and more dark sector asymmetry gets transferred into neutrinos. The right panel of Fig. 4 shows  $\Delta N_{\text{eff}}$  versus DM mass parameter space while different shapes of points indicating the prospect of GW discovery in terms of signal to noise ratio (SNR). The SNR is defined as [109]

$$\rho = \sqrt{\tau \int_{f_{\text{min}}}^{f_{\text{max}}} df \left[ \frac{\Omega_{\text{GW}}(f) h^2}{\Omega_{\text{expt}}(f) h^2} \right]^2}, \quad (12)$$

with  $\tau$  being the observation time for a particular detector, which we consider to be 1 yr. We set the criteria  $\text{SNR} > 5 (> 1)$  for future (present) GW experiments to identify the parameter space. Clearly, the parameter space remains within reach of several GW experiments while at the same time offering complementary probe at future CMB experiments. As expected, lower values of DM mass requires the FOPT to occur at a lower scale to generate the finite temperature window for DM decay, pushing the corresponding peak frequencies towards the PTA ballpark. For the summary plot on the right panel of Fig. 4 and Fig. 5,  $v_D$  is varied from  $10^{-2}$  GeV to  $10^2$  GeV,  $\lambda_{\Phi_1\Phi_2}$  is varied from 1 to 3 and  $Y_{\Delta\chi}$  is varied between  $5 \times 10^{-4}$  and  $5 \times 10^{-2}$ , while  $\lambda_1 = \lambda_2 = 0.01$ ,  $y_1 = 9 \times 10^{-9}$  and  $g_D = 0.4$ . In Fig. 5, we show the zero temperature masses of dark sector particles namely DM and  $\Phi_2$  satisfying all requirements and being within sensitivity of different GW experiments indicated in terms of colour code and point shape.

	$v_D$ (MeV)	$T_c$ (MeV)	$v_c$ (MeV)	$T_n$ (MeV)	$\mu_{\Phi_2}$ (MeV)	$m_{\Phi_2}$ (MeV)	$g_D$	$\lambda_{\Phi_1\Phi_2}$	$\lambda_1$	$\lambda_2$	$\alpha_*$	$\beta/\mathcal{H}_*$	$v_J$	$T_{\text{RH}}$ (MeV)
BP1	20	6.13	18.40	2.57	5	23.30	0.4	2.59	0.01	0.01	1.24	56.06	0.94	2.68
BP2	40	12.27	36.80	5.10	10	45.79	0.4	2.59	0.01	0.01	1.29	51.65	0.94	5.38
BP3	60	17.98	56.40	7.22	20	68.57	0.6	2.39	0.01	0.01	1.65	44.10	0.95	8.12

TABLE I: Benchmark points BP1, BP2, BP3 and other details involved in the GW spectrum calculations.

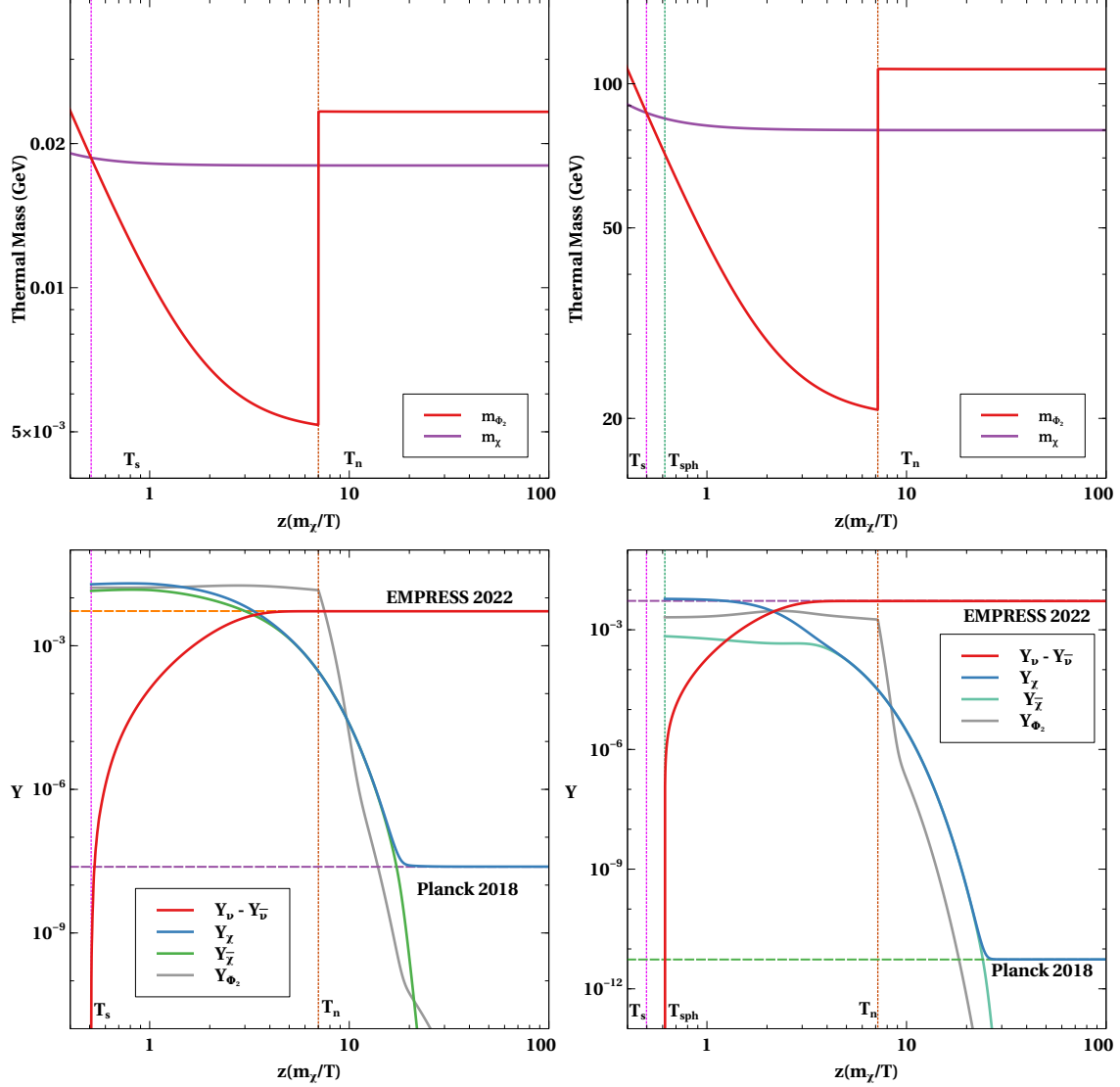


FIG. 2: Top panel: Finite temperature masses of  $\chi$  and  $\Phi_2$  for BP1 (left) and BP6 (right) mentioned in table I, II with  $m_\chi=18\times 10^{-3}$  GeV (left) and  $m_\chi=80$  GeV (right). Bottom panel: Evolution of comoving number densities for BP1 (left) and BP6 (right) with  $y_1 = 7.97 \times 10^{-10}$  (left) and  $y_1 = 1.13 \times 10^{-7}$  (right).

## VI. POSSIBLE UV COMPLETION

In the above discussions, we considered a low energy effective framework with explicit coupling among  $\chi$ ,  $\Phi_2$  and SM neutrinos. Due to the singlet nature of  $\chi$ ,  $\Phi_2$  under the SM gauge symmetry, such a coupling is not allowed. However, it can arise at low energy limit of a UV complete theory. The same UV completion can also explain the origin of dark sector

	$v_D$	$T_c$	$v_c$	$T_n$	$\mu_{\Phi_2}$	$m_{\Phi_2}$	$g_D$	$\lambda_{\Phi_1\Phi_2}$	$\lambda_1$	$\lambda_2$	$\alpha_*$	$\beta/\mathcal{H}_*$	$v_J$	$T_{RH}$
	(GeV)	(GeV)	(GeV)	(GeV)	(GeV)	(GeV)								(GeV)
BP4	1	0.29	0.93	0.11	0.2	1.11	0.6	2.40	0.01	0.01	1.09	62.60	0.93	0.12
BP5	10	2.94	9.30	1.04	0.2	10.29	0.6	2.12	0.01	0.01	0.43	45.62	0.88	1.04
BP6	100	29.70	93.00	11.14	20	107.23	0.6	2.22	0.01	0.01	0.29	50.61	0.85	11.14

TABLE II: Benchmark points BP4, BP5, BP6 and other details involved in the GW spectrum calculations.

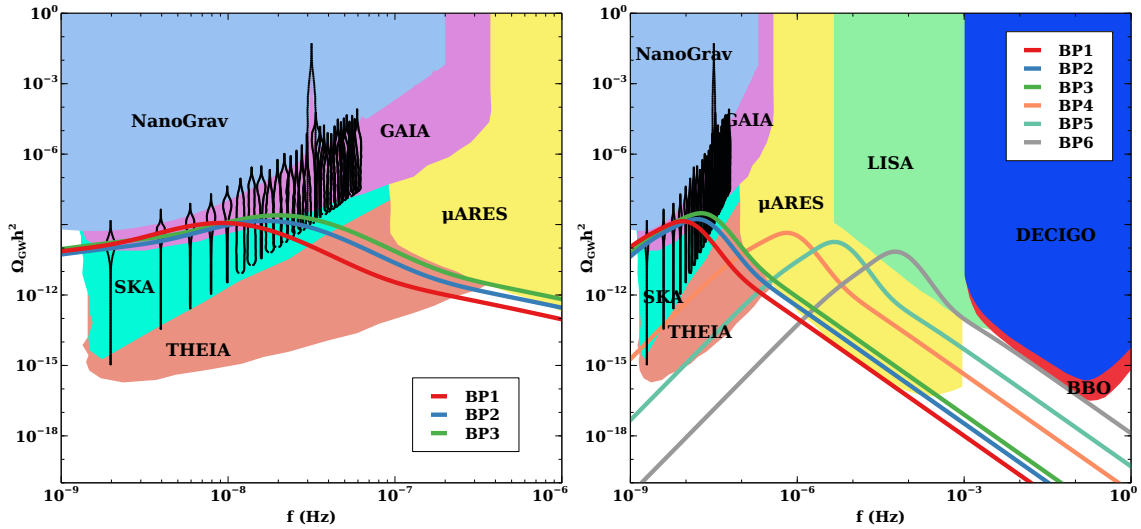


FIG. 3: GW spectrum corresponding to BP1 to BP3 (left) and BP1 to BP6 (right) of table I, II.

asymmetry with possible connections to the baryon asymmetry of the Universe. There have been several proposals for asymmetric DM in the literature [71–73, 76–78, 87, 110–121]. We discuss a simple scenario where singlet right handed neutrinos are included in the SM [110]. If right handed neutrino (RHN) is heavy with a bare mass term of Majorana type, then we have the canonical type-I seesaw [122–126] together with asymmetric DM [110]. The relevant Lagrangian for RHN denoted by  $N$  and dark sector particles  $\chi, \Phi_2$  can be written as

$$-\mathcal{L} \supset y_D \bar{L} \tilde{H} N + y_\chi \bar{\chi} \Phi_2 N + \frac{1}{2} M_N \bar{N}^c N + m_\chi \bar{\chi} \chi + \text{h.c.} \quad (13)$$

The with two or more copies of RHNs, the CP violating out-of-equilibrium decay of the lightest RHN  $N \rightarrow LH, N \rightarrow \chi \Phi_2$  lead to production of asymmetries in lepton and dark sectors respectively. Depending upon the parameters, it is possible to have these two asymmetries

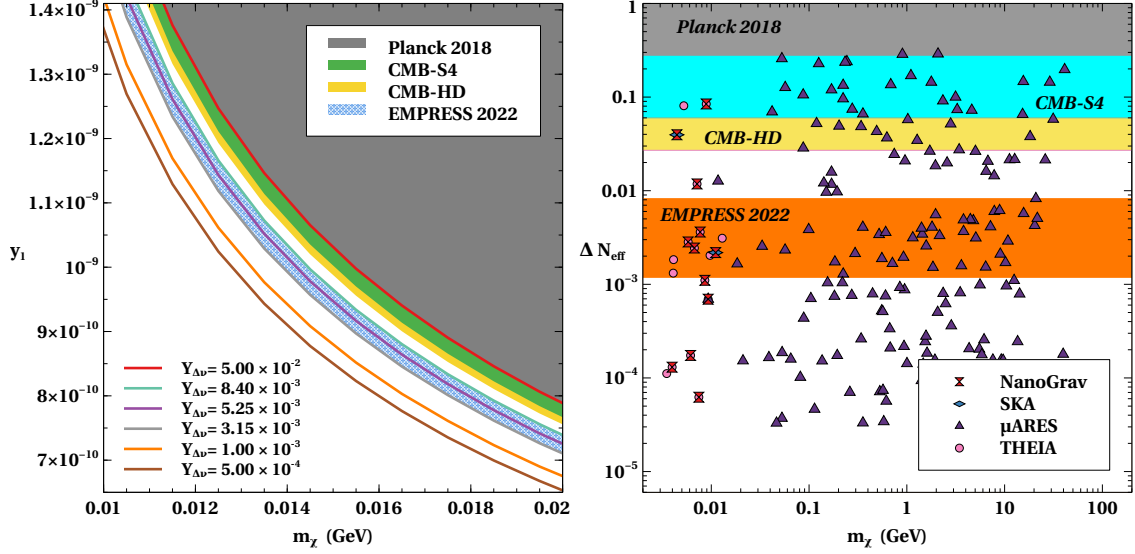


FIG. 4: Left panel: Dark matter mass versus effective Yukawa coupling  $y_1$  for different residual neutrino asymmetry in case of BP1 given in table I. Right panel: Parameter space in  $m_\chi$ - $\Delta N_{\text{eff}}$  plane with color code indicating SNR greater than 5 for future experiments and greater than 1 for ongoing experiments.

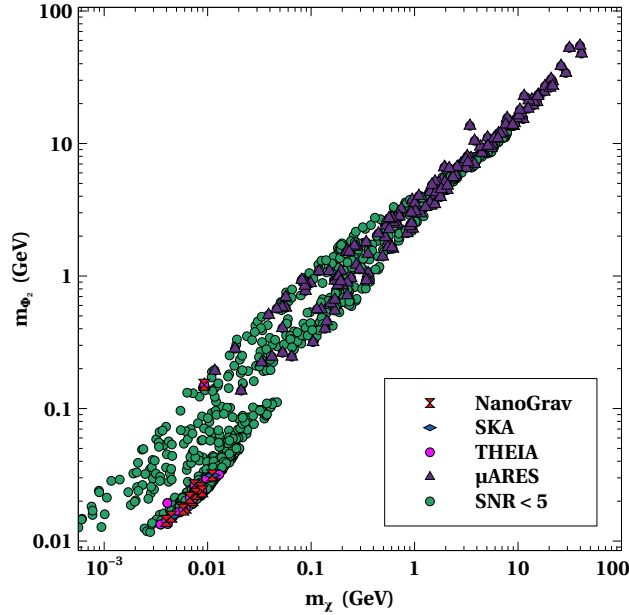


FIG. 5: Parameter space in  $m_\chi$ - $m_{\Phi_2}$  plane with colour code indicating SNR greater than 5 for future experiments and greater than 1 for ongoing experiments.

differ by order of magnitudes [110]. Therefore, the lepton sector asymmetry can be small which gets converted into the observed baryon asymmetry via electroweak sphalerons [127]. On the other hand, DM can have a large asymmetry till it gets partially transferred to the neutrino sector below sphaleron decoupling temperature. After the electroweak symmetry breaking, the heavy RHN mixes with the active neutrinos and which opens up a effective interaction  $y_1 \bar{\chi} \Phi_2 \nu$ , where  $y_1 \sim y_\chi \theta_{\nu N}$  with  $\theta_{\nu N}$  being the active-sterile neutrino mixing angle. While we outline only one such UV completions, we can also consider other scenarios based on other seesaw models like type-II seesaw [126, 128–131], type-III seesaw [132], radiative seesaw [133, 134] or other ways of generating asymmetries like Affleck-Dine mechanism [68]. While these alternate UV completions have different phenomenological consequences, we confine ourselves to the low energy limit only in this work.

## VII. CONCLUSION

We have proposed a mechanism to produce large neutrino asymmetry at low scale from dark matter decay. While dark matter is cosmologically stable, it can decay in the early Universe due to finite temperature effects and if DM is asymmetric like the visible matter, its decay into light neutrinos can transfer some of the dark sector asymmetries into neutrinos. The decay of DM is enabled in the vicinity of a first order phase transition which leads to sharp change in one of the dark sector particle's mass. The large neutrino asymmetry can have interesting cosmological consequences like altering light nuclei abundance which can solve the recently reported Helium-4 anomaly. Such asymmetry can also lead to observable  $\Delta N_{\text{eff}}$  at future CMB experiments. In order to be in agreement with the observed baryon asymmetry, such decay of DM and hence the FOPT are required to occur below the electroweak scale. This keeps the corresponding gravitational wave peak frequencies in nHz-mHz ballpark. Due to the presence of new physics below the electroweak scale, the model can have other detection prospects which we do not discuss here. Asymmetric DM with new gauge interactions can give rise DM self-interactions motivated from small-scale structure problems of cold DM. Additionally, such gauge portal interactions also open up interesting direct detection prospects which we discuss briefly in appendix B.

## Acknowledgments

The work of D.B. is supported by the Science and Engineering Research Board (SERB), Government of India grants MTR/2022/000575 and CRG/2022/000603. The work of N.D. is supported by the Ministry of Education, Government of India via the Prime Minister's Research Fellowship (PMRF) December 2021 scheme.

## Appendix A: Details of FOPT and Gravitational Waves

The dark sector went through a first order phase transition driven by scalar  $\Phi_1$  and the tree level scalar potential can be written as

$$V(\Phi_1, \Phi_2) = \lambda_1 \left( |\Phi_1|^2 - \frac{v_D^2}{2} \right)^2 + \mu_{\Phi_2}^2 |\Phi_2|^2 + \lambda_2 |\Phi_2|^4 + \lambda_{\Phi_1 \Phi_2} |\Phi_1|^2 |\Phi_2|^2. \quad (\text{A1})$$

Here,  $v_D$  is the vacuum expectation value (VEV) of the singlet scalar  $\Phi_1 (\equiv (\phi_1 + v_D + i\phi_g)/\sqrt{2})$ . The Coleman-Weinberg (CW) potential [80] can be written as

$$V_{\text{CW}}(\phi_1) = \frac{1}{(8\pi)^2} \sum_{i=\Phi_1, \Phi_2, Z_D} n_i M_i^4(\phi_1) \left\{ \log \left( \frac{M_i^2(\phi_1)}{v_D^2} \right) - C_i \right\} \quad (\text{A2})$$

where,  $n_{\Phi_1} = 2$ ,  $n_{\Phi_2} = 2$  and  $n_{Z_D} = 3$  and  $C_{\Phi_1, \Phi_2} = \frac{3}{2}$ ,  $C_{Z_D} = \frac{5}{6}$ . The physical field-dependent masses of particles coupled to  $\Phi_1$  are

$$M_{\Phi_2}^2(\phi_1) = \mu_{\Phi_2}^2 + \frac{\lambda_{\Phi_1 \Phi_2} \phi_1^2}{2} \quad \text{and} \quad M_{Z_D}^2(\phi_1) = g_D^2 \phi_1^2.$$

Now, the thermal contributions [81, 82] can be expressed as

$$V_T(\phi_1, T) = \sum_{i=\Phi_1, \Phi_2, Z_D} \frac{n_i T^4}{2\pi^2} J_B \left( \frac{M_i^2(\phi_1)}{T^2} \right) \quad (\text{A3})$$

where

$$J_B(x) = \int_0^\infty dy y^2 \log[1 - e^{-\sqrt{y^2 + x^2}}].$$

In the thermal contribution, the Daisy corrections [135–137] are also added to improve perturbative expansion following Arnold-Espinosa method [137] where  $V_{\text{thermal}}(\phi_1, T) = V_T(\phi_1, T) + V_{\text{daisy}}(\phi_1, T)$ . The Daisy contribution can be written as

$$V_{\text{daisy}}(\phi_1, T) = -\frac{T}{2\pi^2} \sum_{i=\Phi_1, \Phi_2, Z_D} n_i [M_i^3(\phi_1, T) - M_i^3(\phi_1)] \quad (\text{A4})$$

where,  $M_i^2(\phi_1, T) = M_i^2(\phi_1) + \Pi_i(T)$  and the relevant thermal masses are

$$\begin{aligned} M_{\Phi_1}^2(\phi_1, T) &= M_{\Phi_1}^2(\phi_1) + \left( \frac{\lambda_{\Phi_1}}{4} + \frac{\lambda_{\Phi_1\Phi_2}}{12} + \frac{g_D^2}{4} \right) T^2, \\ M_{\Phi_2}^2(\phi_1, T) &= M_{\Phi_2}^2(\phi_1) + \left( \frac{\lambda_{\Phi_2}}{4} + \frac{\lambda_{\Phi_1\Phi_2}}{12} + \frac{g_D^2}{4} \right) T^2, \\ M_{Z_D}^2(\phi_1, T) &= M_{Z_D}^2(\phi_1) + g_D^2 T^2. \end{aligned}$$

Hence, the effective potential at finite temperature can be written as

$$V_{\text{eff}}(\phi_1, T) = V_{\text{tree}}(\phi_1) + V_{\text{CW}}(\phi_1) + V_{\text{thermal}}(\phi_1, T). \quad (\text{A5})$$

The above effective potential shows different profiles depending on the temperature. When the temperature reaches a critical point, the potential develops two identical minima separated by a barrier. Below the critical temperature, the non-zero minimum becomes the true vacuum, while the zero minimum becomes the false vacuum. Due to the presence of the barrier, the Universe remains in the false vacuum, and then transitions from the false vacuum to the true vacuum by tunneling through the barrier. The rate of tunneling per unit time per unit volume can be estimated as  $\Gamma(T) = \mathcal{A}(T)e^{-S_3(T)/T}$ , where  $\mathcal{A}(T) \sim T^4$  and  $S_3$  is Euclidean action. Here, the Hubble parameter is given by  $\mathcal{H}(T) \simeq 1.66\sqrt{g_*}T^2/M_{\text{Pl}}$  with  $g_*$  being the dof of the radiation component. The energy difference between the true and the false vacuum is  $\Delta V_{\text{eff}} \equiv V_{\text{eff}}(\phi_{\text{false}}, T) - V_{\text{eff}}(\phi_{\text{true}}, T)$ . The amount of vacuum energy released during FOPT can be parameterized as  $\alpha_* = \frac{\epsilon_*}{\rho_{\text{rad}}}$ , where radiation energy density of the Universe,  $\rho_{\text{rad}} = g_*\pi^2 T^4/30$  and  $\epsilon_* = [\Delta V_{\text{eff}} - \frac{T}{4} \frac{\partial \Delta V_{\text{eff}}}{\partial T}]_{T=T_n}$ . The inverse duration of FOPT is defined as  $\frac{\beta}{\mathcal{H}(T)_*} \simeq T \frac{d}{dT} \left( \frac{S_3}{T} \right) |_{T=T_n}$ . In this work to calculate the Euclidean action, we fitted the effective potential to a generic potential for which action calculations are described in [84]. This prescription of action estimation is described with details in [27].

As the FOPT progresses, bubbles of true vacuum form and expand to cover the whole Universe. Then these bubbles start to collide with each other and generate stochastic gravitational waves. The gravitational waves are produced from three primary sources: bubble collisions, sound waves in the plasma, and turbulence due to MHD of the plasma. Now, considering these three contributions to GW production, the corresponding GW power spectrum can be written as [138]

$$\Omega_{\text{GW}}(f) = \Omega_{\phi}(f) + \Omega_{\text{sw}}(f) + \Omega_{\text{turb}}(f). \quad (\text{A6})$$



Considering bubble collision as one of the source, the spectrum can be written as [139–141]

$$\Omega_\phi h^2 = 1.67 \times 10^{-5} \left(\frac{100}{g_*}\right)^{1/3} \left(\frac{\mathcal{H}_*}{\beta}\right)^2 \left(\frac{\kappa_\phi \alpha_*}{1 + \alpha_*}\right)^2 \frac{A(a+b)^c}{\left[b(f/f_{\text{peak}}^\phi)^{-a/c} + a(f/f_{\text{peak}}^\phi)^{b/c}\right]^c}, \quad (\text{A7})$$

where,  $a = 2.41, b = 2.42, c = 4.08$  and  $A = 5.13 \times 10^{-2}$  and the peak frequency being

$$f_{\text{peak}}^\phi = 2.02 \times 10^{-6} \text{Hz} \left(\frac{g_*}{100}\right)^{1/6} \left(\frac{T_n}{100 \text{ GeV}}\right) \left(\frac{\beta}{\mathcal{H}_*}\right). \quad (\text{A8})$$

During bubble collision, the energy transfer can be parameterised by the efficiency factor  $\kappa_\phi$ , [142]

$$\kappa_\phi = \frac{1}{1 + 0.715\alpha_*} \left(0.715\alpha_* + \frac{4}{27} \sqrt{\frac{3\alpha_*}{2}}\right). \quad (\text{A9})$$

The Jouguet velocity for bubble can be written as  $v_J = \frac{1/\sqrt{3} + \sqrt{\alpha_*^2 + 2\alpha_*/3}}{1 + \alpha_*}$  [143] and the bubble wall velocity can be estimated as [144]

$$v_w = \begin{cases} \sqrt{\frac{\Delta V_{\text{eff}}}{\alpha_* \rho_{\text{rad}}}} & \text{if } \sqrt{\frac{\Delta V_{\text{eff}}}{\alpha_* \rho_{\text{rad}}}} < v_J \\ 1 & \text{if } \sqrt{\frac{\Delta V_{\text{eff}}}{\alpha_* \rho_{\text{rad}}}} \geq v_J. \end{cases} \quad (\text{A10})$$

The GW spectrum generated from the sound wave in the plasma can be written as [140]

$$\Omega_{\text{sw}} h^2 = 2.59 \times 10^{-6} \left(\frac{100}{g_*}\right)^{1/3} \left(\frac{\mathcal{H}_*}{\beta}\right) \left(\frac{\kappa_{\text{sw}} \alpha_*}{1 + \alpha_*}\right)^2 v_w \frac{7^{3.5} (f/f_{\text{peak}}^{\text{sw}})^3}{(4 + 3(f/f_{\text{peak}}^{\text{sw}})^2)^{3.5}} \Upsilon. \quad (\text{A11})$$

The corresponding peak frequency is given by

$$f_{\text{peak}}^{\text{sw}} = 8.9 \times 10^{-6} \text{Hz} \left(\frac{g_*}{100}\right)^{1/6} \frac{1}{v_w} \left(\frac{T_n}{100 \text{ GeV}}\right) \left(\frac{\beta}{\mathcal{H}_*}\right) \left(\frac{z_p}{10}\right). \quad (\text{A12})$$

The efficiency factor for sound waves is [143]

$$\kappa_{\text{sw}} = \frac{\alpha_*}{0.73 + 0.083\sqrt{\alpha_*} + \alpha_*}. \quad (\text{A13})$$

Here,  $\Upsilon = 1 - \frac{1}{\sqrt{1 + 2\tau_{\text{sw}}\mathcal{H}_*}}$  is a suppression factor [145] where  $\tau_{\text{sw}} \sim R_*/\bar{U}_f$ , mean bubble separation,  $R_* = (8\pi)^{1/3} v_w \beta$  and rms fluid velocity,  $\bar{U}_f = \sqrt{3\kappa_{\text{sw}}\alpha_*/4(1 + \alpha_*)}$ ;  $z_p \sim 10$ . The spectrum generated by the turbulence in the plasma is given by [140, 141, 146]

$$\Omega_{\text{turb}} h^2 = 3.35 \times 10^{-4} \left(\frac{100}{g_*}\right)^{1/3} \left(\frac{\mathcal{H}_*}{\beta}\right) \left(\frac{\kappa_{\text{turb}} \alpha_*}{1 + \alpha_*}\right)^{1.5} v_w \frac{(f/f_{\text{peak}}^{\text{turb}})^3}{(1 + f/f_{\text{peak}}^{\text{turb}})^{3.6} (1 + 8\pi f/h_*)}, \quad (\text{A14})$$

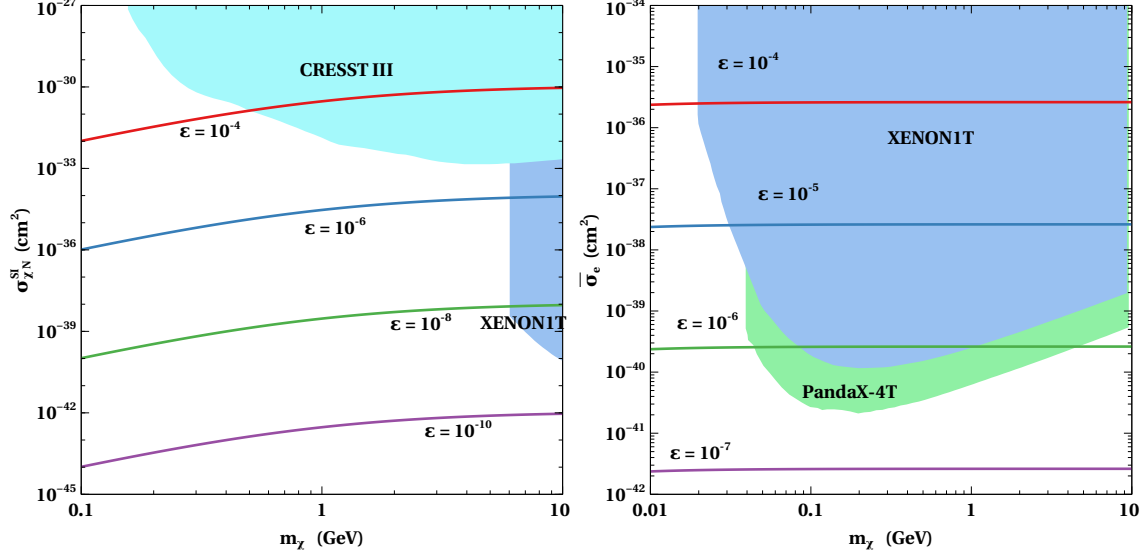


FIG. 6: Left panel: Variation of DM-nucleon elastic scattering cross section with DM mass for different choices of the kinetic mixing parameter. Right panel: Same as the left panel but for DM-electron scattering. For both the panels,  $m_{Z_D} = 8 \times 10^{-3}$  GeV and  $g_D = 0.6$ .

with the peak frequency being [146]

$$f_{\text{peak}}^{\text{turb}} = 2.7 \times 10^{-5} \text{Hz} \left( \frac{g_*}{100} \right)^{1/6} \frac{1}{v_w} \left( \frac{T_n}{100 \text{ GeV}} \right) \left( \frac{\beta}{\mathcal{H}_*} \right). \quad (\text{A15})$$

The efficiency factor for turbulence is  $\kappa_{\text{turb}} \simeq 0.1 \kappa_{\text{sw}}$  [146] and

$$h_* = 1.65 \times 10^{-5} \text{Hz} \left( \frac{g_*}{100} \right)^{1/6} \left( \frac{T_n}{100 \text{ GeV}} \right). \quad (\text{A16})$$

## Appendix B: Direct detection of light DM

The kinetic mixing of  $Z$ - $Z_D$  made possible to probe dark matter through elastic scattering with nucleons in direct detection experiments like CRESST III [147], XENON1T [148] etc. The spin independent DM-nucleon cross section for the experiment target nucleus with atomic number  $Z$  and mass number  $A$  can be written [149] as

$$\sigma_{\chi N}^{SI} = \frac{g^2 g_D^2 \epsilon^2 \mu_{\chi N}^2}{\pi m_{Z_D}^4} \frac{(Z f_p + (A - Z) f_n)^2}{A^2} \quad (\text{B1})$$

where,  $\mu_{\chi N} = \frac{m_\chi m_N}{(m_\chi + m_N)}$  is the reduced mass of DM-nucleon,  $\epsilon$  is  $Z$ - $Z_D$  kinetic mixing,  $f_p$  is interaction strength of proton and  $f_n$  is interaction strength of neutron.

However, the dark matter electron scattering in direct detection experiments XENON1T [148], PandaX-4T [150] can also provide bound on DM mass. The DM-electron reference cross section [151, 152] is given by

$$\bar{\sigma}_e = \frac{16\pi\alpha\alpha_D\epsilon^2\mu_{\chi e}^2}{m_{Z_D}^4} \quad (\text{B2})$$

where,  $\alpha$  is fine structure constant,  $\alpha_D = g_D^2/4\pi$ ,  $\mu_{\chi e} = \frac{m_\chi m_e}{(m_\chi + m_e)}$  is reduced mass of DM-electron. The variation of DM-nucleon and DM-electron scattering cross section with DM mass in the range of our interest is shown in Fig. 6.

- 
- [1] **Particle Data Group** Collaboration, P. A. Zyla et al., *Review of Particle Physics*, *PTEP* **2020** (2020), no. 8 083C01.
- [2] **Planck** Collaboration, N. Aghanim et al., *Planck 2018 results. VI. Cosmological parameters*, [arXiv:1807.06209](#).
- [3] **Planck** Collaboration, N. Aghanim et al., *Planck 2018 results. VI. Cosmological parameters*, *Astron. Astrophys.* **641** (2020) A6, [[arXiv:1807.06209](#)]. [Erratum: *Astron. Astrophys.* 652, C4 (2021)].
- [4] E. W. Kolb and M. S. Turner, *The Early Universe*, vol. 69. 1990.
- [5] G. Jungman, M. Kamionkowski, and K. Griest, *Supersymmetric dark matter*, *Phys. Rept.* **267** (1996) 195–373, [[hep-ph/9506380](#)].
- [6] G. Bertone, D. Hooper, and J. Silk, *Particle dark matter: Evidence, candidates and constraints*, *Phys. Rept.* **405** (2005) 279–390, [[hep-ph/0404175](#)].
- [7] J. L. Feng, *Dark Matter Candidates from Particle Physics and Methods of Detection*, *Ann. Rev. Astron. Astrophys.* **48** (2010) 495–545, [[arXiv:1003.0904](#)].
- [8] G. Arcadi, M. Dutra, P. Ghosh, M. Lindner, Y. Mambrini, M. Pierre, S. Profumo, and F. S. Queiroz, *The waning of the WIMP? A review of models, searches, and constraints*, *Eur. Phys. J. C* **78** (2018), no. 3 203, [[arXiv:1703.07364](#)].
- [9] L. Roszkowski, E. M. Sessolo, and S. Trojanowski, *WIMP dark matter candidates and searches—current status and future prospects*, *Rept. Prog. Phys.* **81** (2018), no. 6 066201, [[arXiv:1707.06277](#)].
- [10] S. Weinberg, *Cosmological Production of Baryons*, *Phys. Rev. Lett.* **42** (1979) 850–853.

- [11] E. W. Kolb and S. Wolfram, *Baryon Number Generation in the Early Universe*, *Nucl. Phys.* **B172** (1980) 224. [Erratum: *Nucl. Phys.*B195,542(1982)].
- [12] M. Fukugita and T. Yanagida, *Baryogenesis Without Grand Unification*, *Phys. Lett.* **B174** (1986) 45–47.
- [13] **LZ** Collaboration, J. Aalbers et al., *First Dark Matter Search Results from the LUX-ZEPLIN (LZ) Experiment*, *Phys. Rev. Lett.* **131** (2023), no. 4 041002, [[arXiv:2207.03764](#)].
- [14] **LZ** Collaboration, S. Haselschwardt, *New Dark Matter Search Results from the LUX-ZEPLIN (LZ) Experiment, Plenary Talk at TeVPA 2024*.
- [15] E. Hall, T. Konstandin, R. McGehee, H. Murayama, and G. Servant, *Baryogenesis From a Dark First-Order Phase Transition*, *JHEP* **04** (2020) 042, [[arXiv:1910.08068](#)].
- [16] J. A. Dror, T. Hiramatsu, K. Kohri, H. Murayama, and G. White, *Testing the Seesaw Mechanism and Leptogenesis with Gravitational Waves*, *Phys. Rev. Lett.* **124** (2020), no. 4 041804, [[arXiv:1908.03227](#)].
- [17] S. Blasi, V. Brdar, and K. Schmitz, *Fingerprint of low-scale leptogenesis in the primordial gravitational-wave spectrum*, *Phys. Rev. Res.* **2** (2020), no. 4 043321, [[arXiv:2004.02889](#)].
- [18] B. Fornal and B. Shams Es Haghi, *Baryon and Lepton Number Violation from Gravitational Waves*, *Phys. Rev. D* **102** (2020), no. 11 115037, [[arXiv:2008.05111](#)].
- [19] R. Samanta and S. Datta, *Gravitational wave complementarity and impact of NANOGrav data on gravitational leptogenesis: cosmic strings*, [arXiv:2009.13452](#).
- [20] B. Barman, D. Borah, A. Dasgupta, and A. Ghoshal, *Probing high scale Dirac leptogenesis via gravitational waves from domain walls*, *Phys. Rev. D* **106** (2022), no. 1 015007, [[arXiv:2205.03422](#)].
- [21] I. Baldes, S. Blasi, A. Mariotti, A. Sevrin, and K. Turbang, *Baryogenesis via relativistic bubble expansion*, *Phys. Rev. D* **104** (2021), no. 11 115029, [[arXiv:2106.15602](#)].
- [22] A. Azatov, M. Vanvlasselaer, and W. Yin, *Baryogenesis via relativistic bubble walls*, *JHEP* **10** (2021) 043, [[arXiv:2106.14913](#)].
- [23] P. Huang and K.-P. Xie, *Leptogenesis triggered by a first-order phase transition*, [arXiv:2206.04691](#).
- [24] A. Dasgupta, P. S. B. Dev, A. Ghoshal, and A. Mazumdar, *Gravitational Wave Pathway to Testable Leptogenesis*, [arXiv:2206.07032](#).

- [25] B. Barman, D. Borah, S. Jyoti Das, and R. Roshan, *Gravitational wave signatures of PBH-generated baryon-dark matter coincidence*, [arXiv:2212.00052](#).
- [26] S. Datta and R. Samanta, *Gravitational waves-tomography of Low-Scale-Leptogenesis*, *JHEP* **11** (2022) 159, [[arXiv:2208.09949](#)].
- [27] D. Borah, A. Dasgupta, and I. Saha, *Leptogenesis and dark matter through relativistic bubble walls with observable gravitational waves*, *JHEP* **11** (2022) 136, [[arXiv:2207.14226](#)].
- [28] D. Borah, A. Dasgupta, and I. Saha, *LIGO-VIRGO constraints on dark matter and leptogenesis triggered by a first order phase transition at high scale*, [arXiv:2304.08888](#).
- [29] D. Borah, A. Dasgupta, M. Knauss, and I. Saha, *Baryon asymmetry from dark matter decay in the vicinity of a phase transition*, *Phys. Rev. D* **108** (2023), no. 9 L091701, [[arXiv:2306.05459](#)].
- [30] B. Barman, D. Borah, S. Jyoti Das, and I. Saha, *Scale of Dirac leptogenesis and left-right symmetry in the light of recent PTA results*, *JCAP* **10** (2023) 053, [[arXiv:2307.00656](#)].
- [31] E. Hall, T. Konstandin, R. McGehee, and H. Murayama, *Asymmetric matter from a dark first-order phase transition*, *Phys. Rev. D* **107** (2023), no. 5 055011, [[arXiv:1911.12342](#)].
- [32] C. Yuan, R. Brito, and V. Cardoso, *Probing ultralight dark matter with future ground-based gravitational-wave detectors*, *Phys. Rev. D* **104** (2021), no. 4 044011, [[arXiv:2106.00021](#)].
- [33] L. Tsukada, R. Brito, W. E. East, and N. Siemonsen, *Modeling and searching for a stochastic gravitational-wave background from ultralight vector bosons*, *Phys. Rev. D* **103** (2021), no. 8 083005, [[arXiv:2011.06995](#)].
- [34] A. Chatrchyan and J. Jaeckel, *Gravitational waves from the fragmentation of axion-like particle dark matter*, *JCAP* **02** (2021) 003, [[arXiv:2004.07844](#)].
- [35] L. Bian, X. Liu, and K.-P. Xie, *Probing superheavy dark matter with gravitational waves*, *JHEP* **11** (2021) 175, [[arXiv:2107.13112](#)].
- [36] R. Samanta and F. R. Urban, *Testing Super Heavy Dark Matter from Primordial Black Holes with Gravitational Waves*, [arXiv:2112.04836](#).
- [37] D. Borah, S. J. Das, A. K. Saha, and R. Samanta, *Probing Miracle-less WIMP Dark Matter via Gravitational Waves Spectral Shapes*, [arXiv:2202.10474](#).
- [38] A. Azatov, M. Vanvlasselaer, and W. Yin, *Dark Matter production from relativistic bubble walls*, *JHEP* **03** (2021) 288, [[arXiv:2101.05721](#)].
- [39] A. Azatov, G. Barni, S. Chakraborty, M. Vanvlasselaer, and W. Yin, *Ultra-relativistic*

- bubbles from the simplest Higgs portal and their cosmological consequences*,  
[arXiv:2207.02230](#).
- [40] I. Baldes, Y. Gouttenoire, and F. Sala, *Hot and Heavy Dark Matter from Supercooling*,  
[arXiv:2207.05096](#).
- [41] D. Borah, S. Jyoti Das, R. Samanta, and F. R. Urban, *PBH-infused seesaw origin of matter and unique gravitational waves*, [arXiv:2211.15726](#).
- [42] D. Borah, S. Jyoti Das, and R. Roshan, *Probing high scale seesaw and PBH generated dark matter via gravitational waves with multiple tilts*, [arXiv:2208.04965](#).
- [43] H. Shibuya and T. Toma, *Impact of first-order phase transitions on dark matter production in the scotogenic model*, *JHEP* **11** (2022) 064, [[arXiv:2207.14662](#)].
- [44] D. Borah, S. Jyoti Das, and R. Samanta, *Imprint of inflationary gravitational waves and WIMP dark matter in pulsar timing array data*, *JCAP* **03** (2024) 031, [[arXiv:2307.00537](#)].
- [45] D. Borah, S. Jyoti Das, and I. Saha, *Dark matter from phase transition generated PBH evaporation with gravitational waves signatures*, *Phys. Rev. D* **110** (2024), no. 3 035014, [[arXiv:2401.12282](#)].
- [46] A. Adhikary, D. Borah, S. Mahapatra, I. Saha, N. Sahu, and V. Thounaojam, *Rescuing thermally under-abundant dark matter with a first-order phase transition*,  
[arXiv:2405.17564](#).
- [47] P. Fileviez Pérez, C. Murgui, and A. D. Plascencia, *Neutrino-Dark Matter Connections in Gauge Theories*, *Phys. Rev.* **D100** (2019), no. 3 035041, [[arXiv:1905.06344](#)].
- [48] D. Nanda and D. Borah, *Connecting Light Dirac Neutrinos to a Multi-component Dark Matter Scenario in Gauged  $B - L$  Model*, *Eur. Phys. J. C* **80** (2020), no. 6 557, [[arXiv:1911.04703](#)].
- [49] C. Han, M. L. López-Ibáñez, B. Peng, and J. M. Yang, *Dirac dark matter in  $U(1)_{B-L}$  with Stueckelberg mechanism*, [arXiv:2001.04078](#).
- [50] D. Mahanta and D. Borah, *Low scale Dirac leptogenesis and dark matter with observable  $\Delta N_{\text{eff}}$* , *Eur. Phys. J. C* **82** (2022), no. 5 495, [[arXiv:2101.02092](#)].
- [51] A. Biswas, D. Borah, and D. Nanda, *Light Dirac neutrino portal dark matter with observable  $\Delta N_{\text{eff}}$* , *JCAP* **10** (2021) 002, [[arXiv:2103.05648](#)].
- [52] D. Borah, P. Das, B. Karmakar, and S. Mahapatra, *Discrete dark matter with light Dirac neutrinos*, [arXiv:2406.17861](#).

- [53] M. Escudero, A. Ibarra, and V. Maura, *Primordial lepton asymmetries in the precision cosmology era: Current status and future sensitivities from BBN and the CMB*, *Phys. Rev. D* **107** (2023), no. 3 035024, [[arXiv:2208.03201](#)].
- [54] G. Mangano, G. Miele, S. Pastor, O. Pisanti, and S. Sarikas, *Constraining the cosmic radiation density due to lepton number with Big Bang Nucleosynthesis*, *JCAP* **03** (2011) 035, [[arXiv:1011.0916](#)].
- [55] G. Mangano, G. Miele, S. Pastor, O. Pisanti, and S. Sarikas, *Updated BBN bounds on the cosmological lepton asymmetry for non-zero  $\theta_{13}$* , *Phys. Lett. B* **708** (2012) 1–5, [[arXiv:1110.4335](#)].
- [56] E. Castorina, U. Franca, M. Lattanzi, J. Lesgourgues, G. Mangano, A. Melchiorri, and S. Pastor, *Cosmological lepton asymmetry with a nonzero mixing angle  $\theta_{13}$* , *Phys. Rev. D* **86** (2012) 023517, [[arXiv:1204.2510](#)].
- [57] X.-D. Shi and G. M. Fuller, *A New dark matter candidate: Nonthermal sterile neutrinos*, *Phys. Rev. Lett.* **82** (1999) 2832–2835, [[astro-ph/9810076](#)].
- [58] M. Drewes et al., *A White Paper on keV Sterile Neutrino Dark Matter*, *JCAP* **01** (2017) 025, [[arXiv:1602.04816](#)].
- [59] A. Mirizzi, N. Saviano, G. Miele, and P. D. Serpico, *Light sterile neutrino production in the early universe with dynamical neutrino asymmetries*, *Phys. Rev. D* **86** (2012) 053009, [[arXiv:1206.1046](#)].
- [60] N. D. Barrie and A. Kobakhidze, *Gravitational Instabilities of the Cosmic Neutrino Background with Non-zero Lepton Number*, *Phys. Lett. B* **772** (2017) 459–463, [[arXiv:1701.00603](#)].
- [61] F. Gao, J. Harz, C. Hati, Y. Lu, I. M. Oldengott, and G. White, *Baryogenesis and first-order QCD transition with gravitational waves from a large lepton asymmetry*, [[arXiv:2407.17549](#)].
- [62] Z. Zeng, S. Yeung, and M.-C. Chu, *Effects of neutrino mass and asymmetry on cosmological structure formation*, *JCAP* **03** (2019) 015, [[arXiv:1808.00357](#)].
- [63] J. March-Russell, H. Murayama, and A. Riotto, *The Small observed baryon asymmetry from a large lepton asymmetry*, *JHEP* **11** (1999) 015, [[hep-ph/9908396](#)].
- [64] V. Domcke, K. Kamada, K. Mukaida, K. Schmitz, and M. Yamada, *New Constraint on Primordial Lepton Flavor Asymmetries*, *Phys. Rev. Lett.* **130** (2023), no. 26 261803,

- [arXiv:2208.03237].
- [65] M. Kawasaki and K. Murai, *Lepton Asymmetric Universe*, arXiv:2203.09713.
- [66] J. McDonald, *Naturally large cosmological neutrino asymmetries in the MSSM*, *Phys. Rev. Lett.* **84** (2000) 4798–4801, [hep-ph/9908300].
- [67] A. Casas, W. Y. Cheng, and G. Gelmini, *Generation of large lepton asymmetries*, *Nucl. Phys. B* **538** (1999) 297–308, [hep-ph/9709289].
- [68] I. Affleck and M. Dine, *A New Mechanism for Baryogenesis*, *Nucl. Phys. B* **249** (1985) 361–380.
- [69] D. Borah and A. Dasgupta, *Large neutrino asymmetry from TeV scale leptogenesis*, *Phys. Rev. D* **108** (2023), no. 3 035015, [arXiv:2206.14722].
- [70] Y. ChoeJo, K. Enomoto, Y. Kim, and H.-S. Lee, *Second leptogenesis: Unraveling the baryon-lepton asymmetry discrepancy*, *JHEP* **03** (2024) 003, [arXiv:2311.16672].
- [71] D. Borah, S. Jyoti Das, and R. Roshan, *Baryon asymmetry from dark matter decay*, *Phys. Rev. D* **108** (2023), no. 7 075025, [arXiv:2305.13367].
- [72] S. Nussinov, *TECHNOCOSMOLOGY: COULD A TECHNIBARYON EXCESS PROVIDE A 'NATURAL' MISSING MASS CANDIDATE?*, *Phys. Lett. B* **165** (1985) 55–58.
- [73] H. Davoudiasl and R. N. Mohapatra, *On Relating the Genesis of Cosmic Baryons and Dark Matter*, *New J. Phys.* **14** (2012) 095011, [arXiv:1203.1247].
- [74] K. Petraki and R. R. Volkas, *Review of asymmetric dark matter*, *Int. J. Mod. Phys. A* **28** (2013) 1330028, [arXiv:1305.4939].
- [75] K. M. Zurek, *Asymmetric Dark Matter: Theories, Signatures, and Constraints*, *Phys. Rept.* **537** (2014) 91–121, [arXiv:1308.0338].
- [76] A. Dutta Banik, R. Roshan, and A. Sil, *Neutrino mass and asymmetric dark matter: study with inert Higgs doublet and high scale validity*, arXiv:2011.04371.
- [77] B. Barman, D. Borah, S. J. Das, and R. Roshan, *Non-thermal origin of asymmetric dark matter from inflaton and primordial black holes*, *JCAP* **03** (2022), no. 03 031, [arXiv:2111.08034].
- [78] Y. Cui and M. Shamma, *WIMP Cogenesis for Asymmetric Dark Matter and the Baryon Asymmetry*, *JHEP* **12** (2020) 046, [arXiv:2002.05170].
- [79] **NANOGrav** Collaboration, G. Agazie et al., *The NANOGrav 15-year Data Set: Evidence for a Gravitational-Wave Background*, arXiv:2306.16213.



- [80] S. R. Coleman and E. J. Weinberg, *Radiative Corrections as the Origin of Spontaneous Symmetry Breaking*, *Phys. Rev. D* **7** (1973) 1888–1910.
- [81] L. Dolan and R. Jackiw, *Symmetry Behavior at Finite Temperature*, *Phys. Rev. D* **9** (1974) 3320–3341.
- [82] M. Quiros, *Finite temperature field theory and phase transitions*, in *ICTP Summer School in High-Energy Physics and Cosmology*, pp. 187–259, 1, 1999. [hep-ph/9901312](#).
- [83] A. D. Linde, *Fate of the False Vacuum at Finite Temperature: Theory and Applications*, *Phys. Lett. B* **100** (1981) 37–40.
- [84] F. C. Adams, *General solutions for tunneling of scalar fields with quartic potentials*, *Phys. Rev. D* **48** (1993) 2800–2805, [[hep-ph/9302321](#)].
- [85] W. Buchmuller, P. Di Bari, and M. Plumacher, *Leptogenesis for pedestrians*, *Annals Phys.* **315** (2005) 305–351, [[hep-ph/0401240](#)].
- [86] P. Gondolo and G. Gelmini, *Cosmic abundances of stable particles: Improved analysis*, *Nucl. Phys.* **B360** (1991) 145–179.
- [87] D. E. Kaplan, M. A. Luty, and K. M. Zurek, *Asymmetric Dark Matter*, *Phys. Rev. D* **79** (2009) 115016, [[arXiv:0901.4117](#)].
- [88] Y.-Z. Li and J.-H. Yu, *Revisiting primordial neutrino asymmetries, spectral distortions and cosmological constraints with full neutrino transport*, [arXiv:2409.08280](#).
- [89] G. Mangano, G. Miele, S. Pastor, T. Pinto, O. Pisanti, and P. D. Serpico, *Relic neutrino decoupling including flavor oscillations*, *Nucl. Phys. B* **729** (2005) 221–234, [[hep-ph/0506164](#)].
- [90] E. Grohs, G. M. Fuller, C. T. Kishimoto, M. W. Paris, and A. Vlasenko, *Neutrino energy transport in weak decoupling and big bang nucleosynthesis*, *Phys. Rev. D* **93** (2016), no. 8 083522, [[arXiv:1512.02205](#)].
- [91] P. F. de Salas and S. Pastor, *Relic neutrino decoupling with flavour oscillations revisited*, *JCAP* **1607** (2016), no. 07 051, [[arXiv:1606.06986](#)].
- [92] **DESI** Collaboration, A. G. Adame et al., *DESI 2024 VI: Cosmological Constraints from the Measurements of Baryon Acoustic Oscillations*, [arXiv:2404.03002](#).
- [93] R. H. Cyburt, B. D. Fields, K. A. Olive, and T.-H. Yeh, *Big Bang Nucleosynthesis: 2015*, *Rev. Mod. Phys.* **88** (2016) 015004, [[arXiv:1505.01076](#)].
- [94] K. Abazajian et al., *CMB-S4 Science Case, Reference Design, and Project Plan*,

- [arXiv:1907.04473](#).
- [95] **CMB-HD** Collaboration, S. Aiola et al., *Snowmass2021 CMB-HD White Paper*, [arXiv:2203.05728](#).
- [96] A. Matsumoto et al., *EMPRESS. VIII. A New Determination of Primordial He Abundance with Extremely Metal-Poor Galaxies: A Suggestion of the Lepton Asymmetry and Implications for the Hubble Tension*, [arXiv:2203.09617](#).
- [97] T. Hsyu, R. J. Cooke, J. X. Prochaska, and M. Bolte, *The PHLEK Survey: A New Determination of the Primordial Helium Abundance*, *Astrophys. J.* **896** (June, 2020) 77, [[arXiv:2005.12290](#)].
- [98] E. Aver, K. A. Olive, and E. D. Skillman, *The effects of He I  $\lambda 10830$  on helium abundance determinations*, *JCAP* **07** (2015) 011, [[arXiv:1503.08146](#)].
- [99] Y. I. Izotov, T. X. Thuan, and N. G. Guseva, *A new determination of the primordial He abundance using the He I  $\lambda 10830$  Å emission line: cosmological implications*, *Mon. Not. Roy. Astron. Soc.* **445** (2014), no. 1 778–793, [[arXiv:1408.6953](#)].
- [100] A.-K. Burns, T. M. P. Tait, and M. Valli, *Indications for a Nonzero Lepton Asymmetry in the Early Universe*, [arXiv:2206.00693](#).
- [101] M. L. Bellac, *Thermal Field Theory*. Cambridge Monographs on Mathematical Physics. Cambridge University Press, 3, 2011.
- [102] M. Laine and A. Vuorinen, *Basics of Thermal Field Theory*, vol. 925. Springer, 2016.
- [103] **LISA** Collaboration, P. Amaro-Seoane et al, *Laser Interferometer Space Antenna*, *arXiv e-prints* (Feb., 2017) arXiv:1702.00786, [[arXiv:1702.00786](#)].
- [104] A. Sesana et al., *Unveiling the gravitational universe at  $\mu$ -Hz frequencies*, *Exper. Astron.* **51** (2021), no. 3 1333–1383, [[arXiv:1908.11391](#)].
- [105] J. Garcia-Bellido, H. Murayama, and G. White, *Exploring the Early Universe with Gaia and THEIA*, [arXiv:2104.04778](#).
- [106] A. Weltman et al., *Fundamental physics with the Square Kilometre Array*, *Publ. Astron. Soc. Austral.* **37** (2020) e002, [[arXiv:1810.02680](#)].
- [107] S. Kawamura et al., *The Japanese space gravitational wave antenna DECIGO*, *Class. Quant. Grav.* **23** (2006) S125–S132.
- [108] K. Yagi and N. Seto, *Detector configuration of DECIGO/BBO and identification of cosmological neutron-star binaries*, *Phys. Rev. D* **83** (2011) 044011, [[arXiv:1101.3940](#)].

- [Erratum: Phys.Rev.D 95, 109901 (2017)].
- [109] K. Schmitz, *New Sensitivity Curves for Gravitational-Wave Experiments*,  
[arXiv:2002.04615](#).
- [110] A. Falkowski, J. T. Ruderman, and T. Volansky, *Asymmetric Dark Matter from Leptogenesis*, *JHEP* **05** (2011) 106, [[arXiv:1101.4936](#)].
- [111] U. Patel, L. Malhotra, S. Patra, and U. A. Yajnik, *Cogenesis of visible and dark sector asymmetry in a minimal seesaw framework*, [arXiv:2211.04722](#).
- [112] A. Biswas, S. Choubey, L. Covi, and S. Khan, *Common origin of baryon asymmetry, dark matter and neutrino mass*, *JHEP* **05** (2019) 193, [[arXiv:1812.06122](#)].
- [113] N. Narendra, S. Patra, N. Sahu, and S. Shil, *Baryogenesis via Leptogenesis from Asymmetric Dark Matter and radiatively generated Neutrino mass*, *Phys. Rev. D* **98** (2018), no. 9 095016, [[arXiv:1805.04860](#)].
- [114] N. Nagata, K. A. Olive, and J. Zheng, *Asymmetric Dark Matter Models in  $SO(10)$* , *JCAP* **02** (2017) 016, [[arXiv:1611.04693](#)].
- [115] C. Arina and N. Sahu, *Asymmetric Inelastic Inert Doublet Dark Matter from Triplet Scalar Leptogenesis*, *Nucl. Phys. B* **854** (2012) 666–699, [[arXiv:1108.3967](#)].
- [116] C. Arina, J.-O. Gong, and N. Sahu, *Unifying darko-lepto-genesis with scalar triplet inflation*, *Nucl. Phys. B* **865** (2012) 430–460, [[arXiv:1206.0009](#)].
- [117] C. Arina, R. N. Mohapatra, and N. Sahu, *Co-genesis of Matter and Dark Matter with Vector-like Fourth Generation Leptons*, *Phys. Lett. B* **720** (2013) 130–136, [[arXiv:1211.0435](#)].
- [118] N. Narendra, N. Sahu, and S. Shil, *Dark matter to baryon ratio from scalar triplets decay in type-II seesaw*, *Eur. Phys. J. C* **81** (2021), no. 12 1098, [[arXiv:1910.12762](#)].
- [119] S. Mahapatra, P. K. Paul, N. Sahu, and P. Shukla, *Cogenesis of matter and dark matter from triplet fermion seesaw*, [arXiv:2305.11138](#).
- [120] D. Borah, S. Jyoti Das, and N. Okada, *Affleck-Dine cogenesis of baryon and dark matter*, *JHEP* **05** (2023) 004, [[arXiv:2212.04516](#)].
- [121] D. Borah, S. Mahapatra, P. K. Paul, N. Sahu, and P. Shukla, *Asymmetric self-interacting dark matter with a canonical seesaw model*, *Phys. Rev. D* **110** (2024), no. 3 035033, [[arXiv:2404.14912](#)].
- [122] P. Minkowski,  $\mu \rightarrow e\gamma$  at a Rate of One Out of  $10^9$  Muon Decays?, *Phys. Lett.* **B67** (1977)

- 421–428.
- [123] M. Gell-Mann, P. Ramond, and R. Slansky, *Complex Spinors and Unified Theories*, *Conf. Proc.* **C790927** (1979) 315–321, [[arXiv:1306.4669](#)].
- [124] R. N. Mohapatra and G. Senjanovic, *Neutrino Mass and Spontaneous Parity Violation*, *Phys. Rev. Lett.* **44** (1980) 912.
- [125] J. Schechter and J. W. F. Valle, *Neutrino Masses in  $SU(2) \times U(1)$  Theories*, *Phys. Rev.* **D22** (1980) 2227.
- [126] J. Schechter and J. W. F. Valle, *Neutrino Decay and Spontaneous Violation of Lepton Number*, *Phys. Rev.* **D25** (1982) 774.
- [127] V. A. Kuzmin, V. A. Rubakov, and M. E. Shaposhnikov, *On the Anomalous Electroweak Baryon Number Nonconservation in the Early Universe*, *Phys. Lett.* **155B** (1985) 36.
- [128] R. N. Mohapatra and G. Senjanovic, *Neutrino Masses and Mixings in Gauge Models with Spontaneous Parity Violation*, *Phys. Rev. D* **23** (1981) 165.
- [129] C. Wetterich, *Neutrino Masses and the Scale of B-L Violation*, *Nucl. Phys.* **B187** (1981) 343–375.
- [130] G. Lazarides, Q. Shafi, and C. Wetterich, *Proton Lifetime and Fermion Masses in an  $SO(10)$  Model*, *Nucl. Phys. B* **181** (1981) 287–300.
- [131] B. Brahmachari and R. N. Mohapatra, *Unified explanation of the solar and atmospheric neutrino puzzles in a minimal supersymmetric  $SO(10)$  model*, *Phys. Rev.* **D58** (1998) 015001, [[hep-ph/9710371](#)].
- [132] R. Foot, H. Lew, X. G. He, and G. C. Joshi, *Seesaw Neutrino Masses Induced by a Triplet of Leptons*, *Z. Phys.* **C44** (1989) 441.
- [133] Z.-j. Tao, *Radiative seesaw mechanism at weak scale*, *Phys. Rev. D* **54** (1996) 5693–5697, [[hep-ph/9603309](#)].
- [134] E. Ma, *Common origin of neutrino mass, dark matter, and baryogenesis*, *Mod. Phys. Lett.* **A21** (2006) 1777–1782, [[hep-ph/0605180](#)].
- [135] P. Fendley, *The Effective Potential and the Coupling Constant at High Temperature*, *Phys. Lett. B* **196** (1987) 175–180.
- [136] R. R. Parwani, *Resummation in a hot scalar field theory*, *Phys. Rev. D* **45** (1992) 4695, [[hep-ph/9204216](#)]. [Erratum: *Phys.Rev.D* 48, 5965 (1993)].
- [137] P. B. Arnold and O. Espinosa, *The Effective potential and first order phase transitions:*

- Beyond leading-order*, *Phys. Rev. D* **47** (1993) 3546, [[hep-ph/9212235](#)]. [Erratum: *Phys.Rev.D* 50, 6662 (1994)].
- [138] R.-G. Cai, M. Sasaki, and S.-J. Wang, *The gravitational waves from the first-order phase transition with a dimension-six operator*, *JCAP* **08** (2017) 004, [[arXiv:1707.03001](#)].
- [139] M. Lewicki and V. Vaskonen, *Gravitational waves from bubble collisions and fluid motion in strongly supercooled phase transitions*, *Eur. Phys. J. C* **83** (2023), no. 2 109, [[arXiv:2208.11697](#)].
- [140] P. Athron, C. Balázs, A. Fowlie, L. Morris, and L. Wu, *Cosmological phase transitions: from perturbative particle physics to gravitational waves*, [arXiv:2305.02357](#).
- [141] **LISA Cosmology Working Group** Collaboration, C. Caprini, R. Jinno, M. Lewicki, E. Madge, M. Merchand, G. Nardini, M. Pieroni, A. Roper Pol, and V. Vaskonen, *Gravitational waves from first-order phase transitions in LISA: reconstruction pipeline and physics interpretation*, [arXiv:2403.03723](#).
- [142] M. Kamionkowski, A. Kosowsky, and M. S. Turner, *Gravitational radiation from first order phase transitions*, *Phys. Rev. D* **49** (1994) 2837–2851, [[astro-ph/9310044](#)].
- [143] J. R. Espinosa, T. Konstandin, J. M. No, and G. Servant, *Energy Budget of Cosmological First-order Phase Transitions*, *JCAP* **06** (2010) 028, [[arXiv:1004.4187](#)].
- [144] M. Lewicki, M. Merchand, and M. Zych, *Electroweak bubble wall expansion: gravitational waves and baryogenesis in Standard Model-like thermal plasma*, *JHEP* **02** (2022) 017, [[arXiv:2111.02393](#)].
- [145] H.-K. Guo, K. Sinha, D. Vagie, and G. White, *Phase Transitions in an Expanding Universe: Stochastic Gravitational Waves in Standard and Non-Standard Histories*, [arXiv:2007.08537](#).
- [146] C. Caprini et al., *Science with the space-based interferometer eLISA. II: Gravitational waves from cosmological phase transitions*, *JCAP* **1604** (2016), no. 04 001, [[arXiv:1512.06239](#)].
- [147] **CRESST** Collaboration, A. H. Abdelhameed et al., *First results from the CRESST-III low-mass dark matter program*, *Phys. Rev. D* **100** (2019), no. 10 102002, [[arXiv:1904.00498](#)].
- [148] **XENON** Collaboration, E. Aprile et al., *Light Dark Matter Search with Ionization Signals in XENON1T*, *Phys. Rev. Lett.* **123** (2019), no. 25 251801, [[arXiv:1907.11485](#)].
- [149] D. Borah, M. Dutta, S. Mahapatra, and N. Sahu, *Self-interacting Dark Matter via Right*

*Handed Neutrino Portal*, [arXiv:2110.00021](#).

- [150] **PandaX** Collaboration, S. Li et al., *Search for Light Dark Matter with Ionization Signals in the PandaX-4T Experiment*, *Phys. Rev. Lett.* **130** (2023), no. 26 261001, [[arXiv:2212.10067](#)].
- [151] R. Essig, M. Fernandez-Serra, J. Mardon, A. Soto, T. Volansky, and T.-T. Yu, *Direct Detection of sub-GeV Dark Matter with Semiconductor Targets*, *JHEP* **05** (2016) 046, [[arXiv:1509.01598](#)].
- [152] A. Prabhu and C. Blanco, *Constraints on dark matter-electron scattering from molecular cloud ionization*, *Phys. Rev. D* **108** (2023), no. 3 035035, [[arXiv:2211.05787](#)].